Supporting Information

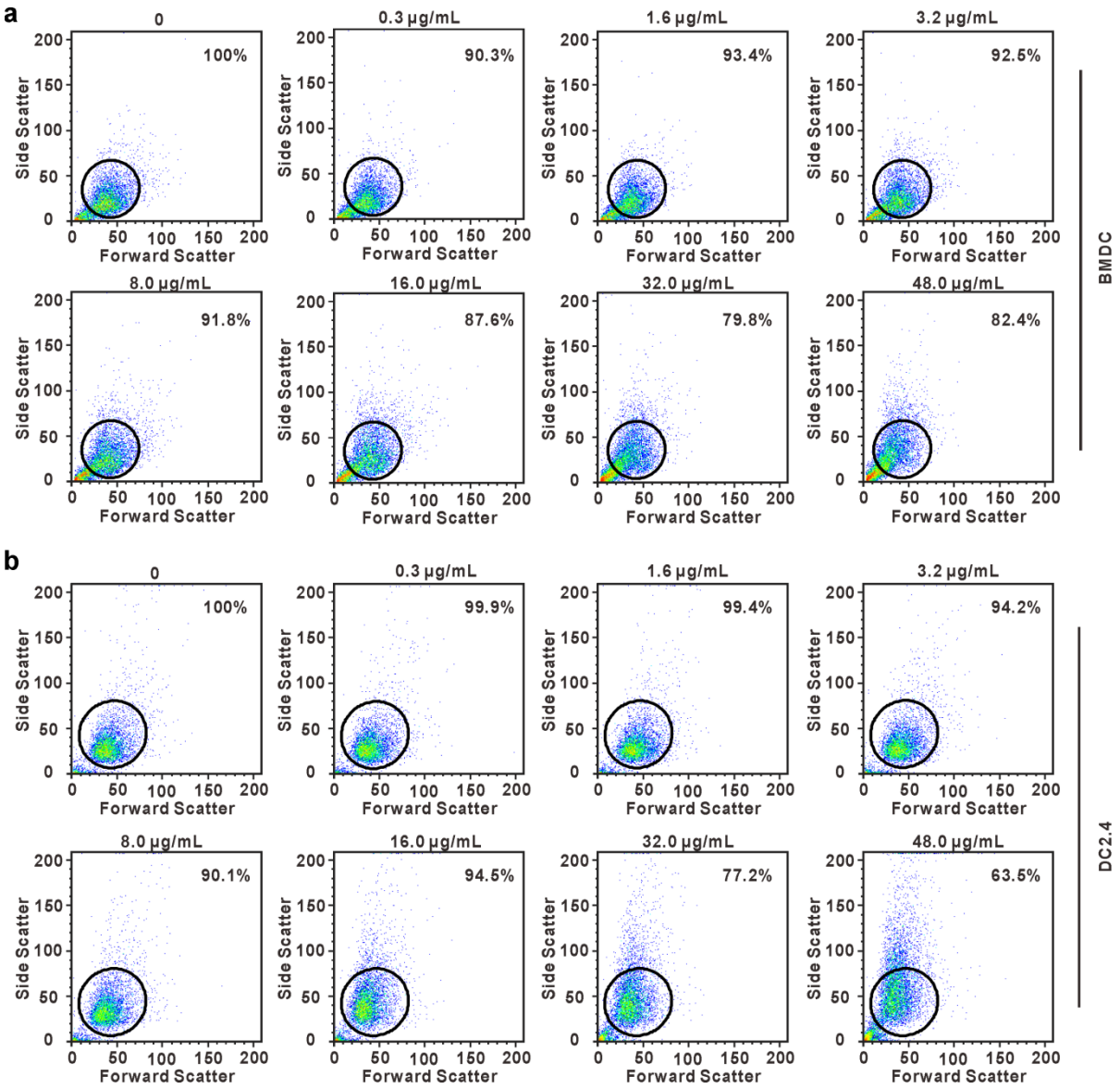

Figure S1. Measurement of morphological changed cells by flow cytometry. Cells were incubated with various concentrations of α-AP-fmNPs (measured by iron concentration) for 24 h and morphological changed cells were determined. a) BMDCs; b) DC2.4 cells.

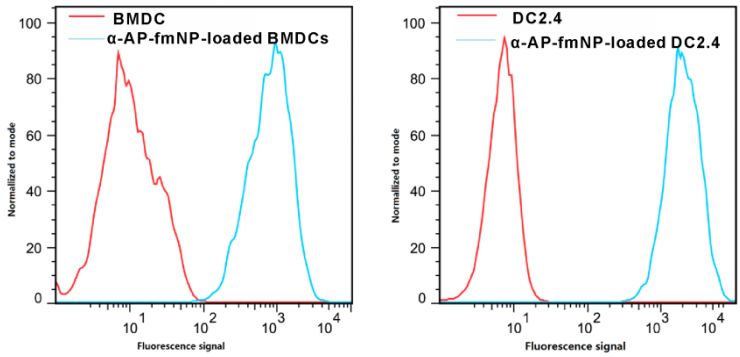

Figure S2. Flow cytometry analysis of the efficiency of BMDCs and DC2.4 cells labeling with α-AP-fmNPs. BMDCs and DC2.4 cells were incubated with 16 μg/mL (measured by iron concentration) α-AP-fmNPs for 6 h, respectively, and were subjected to flow cytometry analysis.

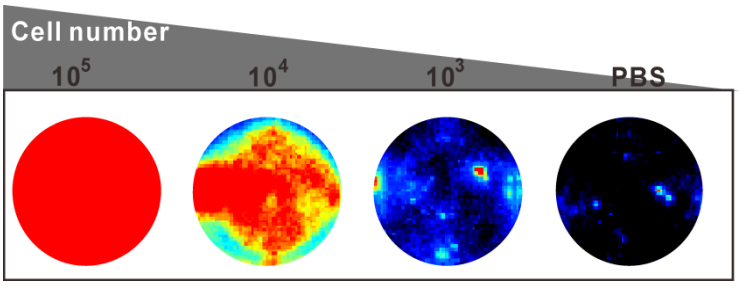

Figure S3. NIR images of α-AP_{gp100}-fmNPs-loaded DC2.4 cells with different cell number. Image shows a concentration-dependent manner.

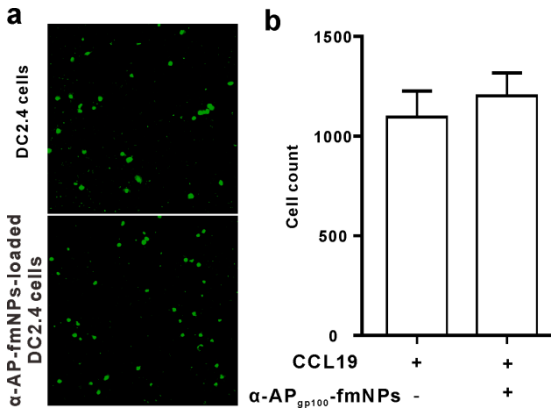

Figure S4. Effect of FAM-α-AP-fmNPs loading on the migration abilities of DC2.4 cells. a) Representative images of migrated DC2.4 cells to the bottom of the chamber observed by confocal imaging. The cells were stained with Hoechst 33258. Both the α-AP-fmNP-loaded DC2.4 cells and DC2.4 cell control groups contained CCL19 in the bottom chamber to facilitate cell migration. b) Statistical analysis of migrated cells. No significant difference was found between DC2.4 cell control and α-AP-fmNP-loaded DC2.4 cells.

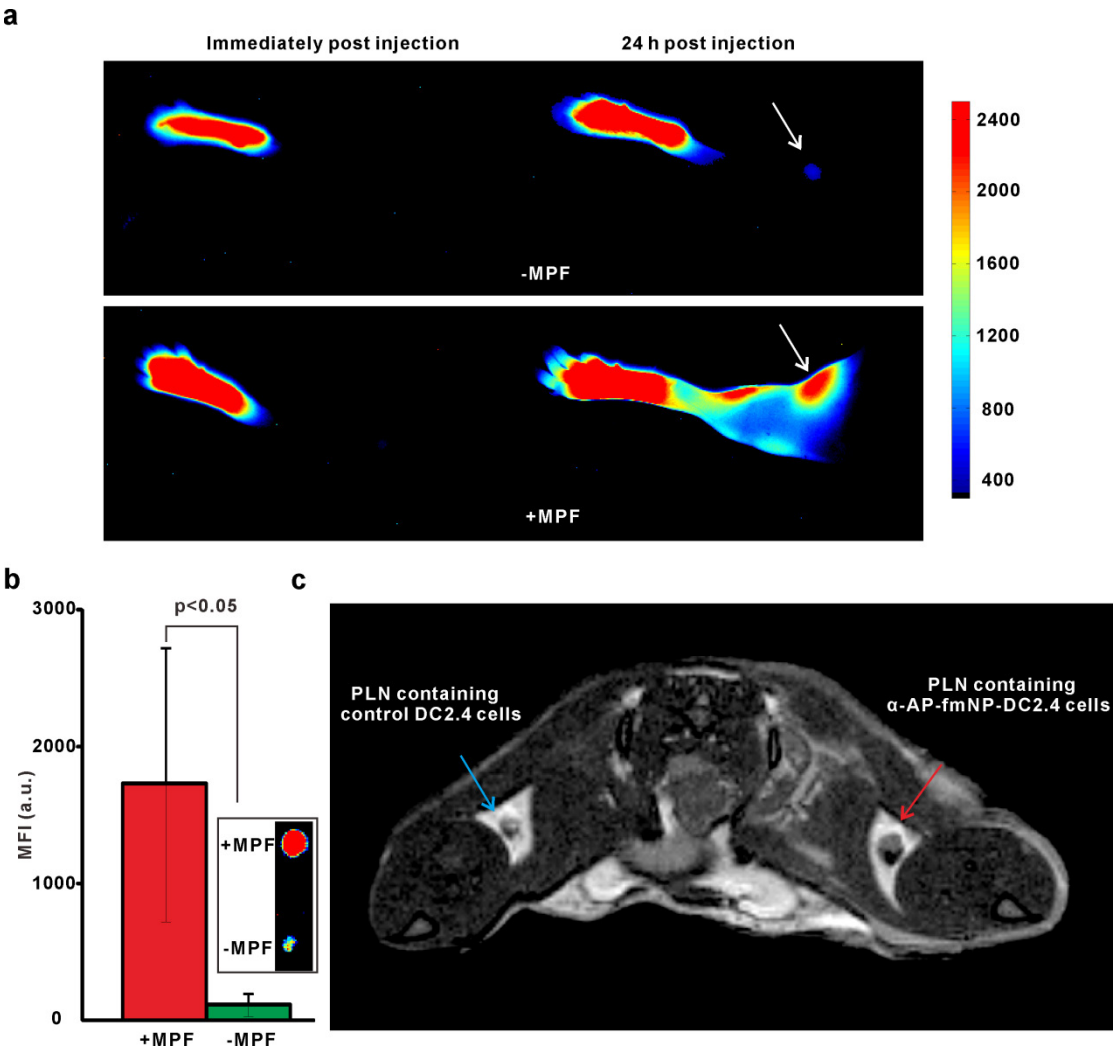

Figure S5. Bimodal imaging of MPF-promoted migration of DC2.4 cells to the LN. a) Optical imaging of DC2.4 cell migration at 0 h and 24 h post-injection in the presence (+MPF, bottom panel) or absence (-MPF, top panel) of magnetic field exposure. b) Average fluorescence measurements and NIR images of dissected PLNs (inset). Data are presented as the mean ± SEM (3–4 mice per group). The experiment was repeated at least three times with similar results. c) Representative MRI images of α-AP-fmNPs-treated mice (blue arrow: DC2.4 cells; red arrow: α-AP-fmNP-loaded DC2.4 cells).

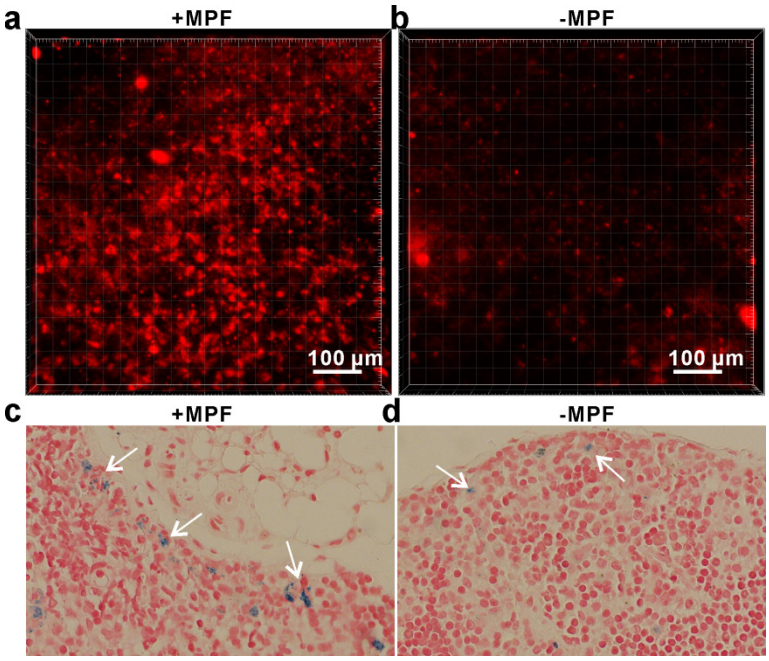

Figure S6. Validation of MPF-assisted migration of DC2.4 cells. a) Confocal images of the dissected LNs in the presence (+MPF, left panel) or (b) absence (-MPF, right panel) of magnetic field exposure. ICG signals in the LNs were acquired. Red color stains for ICG signal. c) Histological analysis of α-AP-fmNPs accumulation in the PLNs by Prussian blue staining in the (c) presence (+MPF) or (d) absence (-MPF) of MPF.

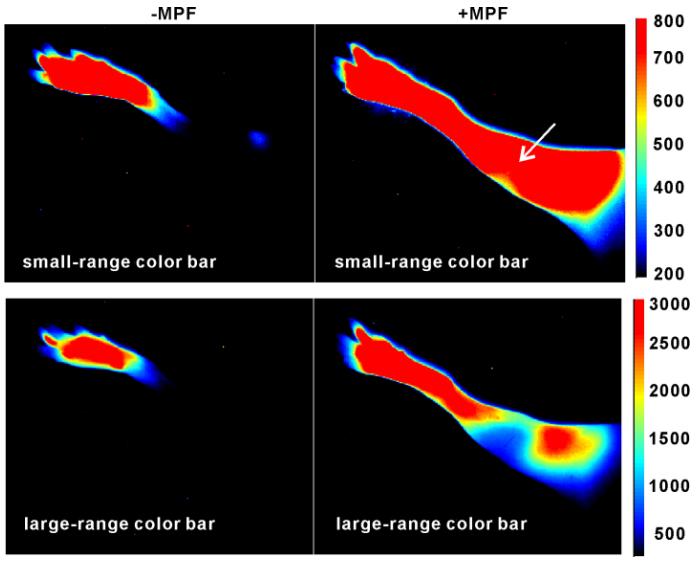

Figure S7. NIR images of the migrated cells displayed with different color bars. Under a relatively low color bar range (fluorescence signal: 200-800), the entire leg of the mouse treated with MPF displayed strong fluorescence signal.

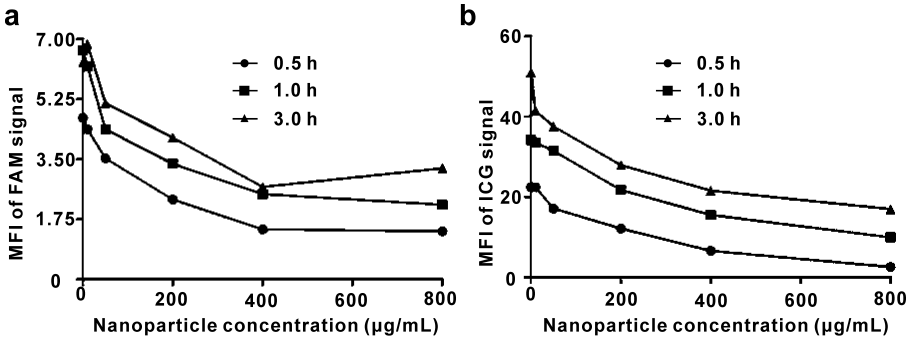

Figure S8. Inhibition of FAM-α-AP-fmNPs uptake by various concentrations of HPPS. a) Measurement of the FAM signal of FAM-α-AP-fmNP-loaded BMDCs. b) Measurement of the ICG signal of α-AP-fmNP-loaded BMDCs.

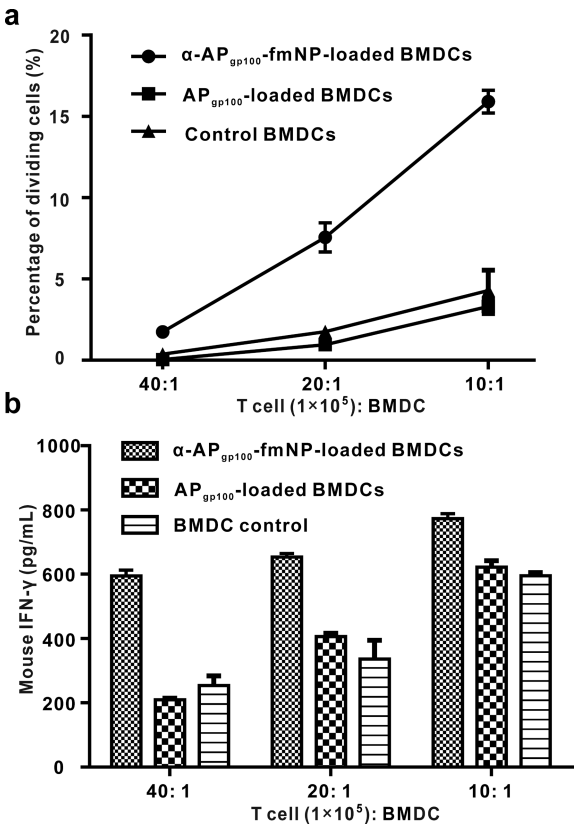

Figure S9. Immune function assessment with a tumor specific antigen gp100. a) *In vitro* gp100-specific $CD8^+$ T cell activation by α-AP_{gp100}-fmNP-loaded DCs. T cells collected from the AP_{gp100}-immunized mice were stained with CFSE and co-cultured with mature BMDCs loaded with AP_{gp100}, PBS, or α-AP_{gp100}-fmNPs at various T cell: DC ratios. T cell proliferation was measured *via* CFSE fluorescence dilution flow cytometry. b) Measurement of IFN-γ concentrations of the supernatants from T cell expansions using ELISA.